

RSC Advances



This is an *Accepted Manuscript*, which has been through the Royal Society of Chemistry peer review process and has been accepted for publication.

Accepted Manuscripts are published online shortly after acceptance, before technical editing, formatting and proof reading. Using this free service, authors can make their results available to the community, in citable form, before we publish the edited article. This *Accepted Manuscript* will be replaced by the edited, formatted and paginated article as soon as this is available.

You can find more information about *Accepted Manuscripts* in the [Information for Authors](#).

Please note that technical editing may introduce minor changes to the text and/or graphics, which may alter content. The journal's standard [Terms & Conditions](#) and the [Ethical guidelines](#) still apply. In no event shall the Royal Society of Chemistry be held responsible for any errors or omissions in this *Accepted Manuscript* or any consequences arising from the use of any information it contains.

Optimized preparation conditions of TiO₂ deposited on SiO₂ solid superacid nanotubes as filler materials

Yuqing Zhang^{1,2,*}, Honglu Zhao^{1,2}

¹*School of Chemical Engineering and Technology, Tianjin University, Tianjin 300072, P R China*

²*Collaborative Innovation Center of Chemical Science and Engineering (Tianjin), Tianjin 300072,
P R China*

Abstract

The preparation conditions perform the important impact on the structure and properties of TiO₂ deposited on SiO₂ solid superacid nanotubes (TSANs). In this paper, the preparation conditions of TSANs such as the molar ratio of Ti/Si, the concentration of sulphuric acid aqueous solution, the dipping time in sulphuric acid aqueous solution and the calcination temperature etc were investigated and optimized, the optimum preparation conditions were finally determined. TSANs were employed as novel filler materials to prepare TSANs/PSF composite membranes with micro reaction locations (MRLs) inside channels and on the surface of composite membranes. TSANs and TSANs/PSF composite membranes were characterized and studied by SEM, TEM, EDX, FT-IR, BET and contact angle of water etc. The results indicate that the thickness of the tube wall is 50 nm, the ratio of length to diameter of TSANs is approximately 23 and SiO₄²⁻/TiO₂-SiO₂ solid superacid nanotube is formed due to a stretching vibration peak of S=O double bond at 1300 cm⁻¹ in FT-IR spectra. The contact angle is declined from 76.5° to 36.5° and oil retention ratio of TSANs/PSF composite membranes reaches 94.2 %, which perform the attractive hydrophilic and anti-fouling properties of TSANs/PSF composite membranes. Therefore,

* Corresponding author: Phone: +86-22-27890470; fax: +86-22-27403389;
E-mail address: zhangyuqing@tju.edu.cn

TSANs are desirable as novel filler materials of PSF membrane to improve its integrated properties.

Key words: Optimized preparation conditions; Silica nanotube; Sulfated TiO₂; Solid superacid; Polysulfone membrane

1. Introduction

The strategy of doping inorganic oxide nanoparticles into polymer membranes to prepare organic-inorganic composite membranes is extremely fascinating. Polysulfone (PSF) membranes have been extensively applied to microfiltration membranes, ultrafiltration membranes, gas separation membranes, pervaporation membranes, because of its outstanding properties such as excellent mechanical strength, good chemical resistance and high thermal stability.¹⁻³ However, due to the hydrophobic characteristic of PSF material, conventional PSF membranes easily suffer serious membrane fouling, which deteriorates membrane performance and shortens membrane life.⁴⁻⁶ In order to solve these drawbacks, various inorganic oxide nanoparticles such as TiO₂, SiO₂, and Al₂O₃ have been broadly employed as filler materials for the synthesis of composite membranes to enhance their performance.⁷⁻⁹ However, further enhancement of the integrated properties of polymer membranes is limited because these inorganic nanoparticles could neither be compatible with polymers along the direction of polymer chains well nor supply excellent anti-compaction capabilities to resist the outer impact forces because they are not rod-shaped or tubal materials with high ratio of length to diameter.

In recent years, with the discovery of carbon nanotubes (CNTs),¹⁰ CNTs have motivated plenty of researchers to explore their potential applications in areas of advanced materials. CNTs are appealing membrane fillers with extraordinary mass transport channels, which have been

studied by various research groups. Several studies have shown successful application of CNTs in a polymer matrix.¹¹⁻¹³ Analogously, silica nanotubes (SNTs) also raise special interest as filler materials because they have many advantages such as hollow structures,¹⁴ high specific surface areas,¹⁵ high ratio of length to diameter,¹⁶ biocompatibility¹⁷ and good anti-compaction strength.¹⁸ So when SNTs are employed as filler materials in the synthesis of SNTs/PSF composite membranes, the composite membranes have better compatibility and good anti-compaction performance.

In addition, membrane fouling is a major obstacle in the widespread application of membrane technology. Through the analysis of membrane fouling mechanism,^{19,20} pollutants are mainly divided into three categories such as inorganic pollutants (metal oxides etc.), microbes and organic pollutants (hydrocarbon and soluble oil etc.).^{21,22} However, the above methods just dope nanomaterials with small size into polymer membranes to enhance their anti-fouling properties by physical interaction on the interface between aqueous solution and composite membranes, but without any chemical reaction. Therefore, in order to introduce chemical reaction, it is significant to design and research a type of novel functional nanomaterials with solid superacid properties, which can form MRLs inside channels and surface of membranes. Sulfated TiO₂ is well known as a solid superacid with 10,000 times Hammett acidity of 100% H₂SO₄,²³ which can decompose inorganic pollutants such as metal oxides or restrain their formation inside channels and surface of membranes, extending the membrane lifespan.²⁴ Moreover, due to the strong acidity of sulfated TiO₂ solid superacid and the inductive effect of S=O bonds, a large number of hydroxyl groups are produced on the surface of sulfated TiO₂ solid superacid, which can improve the hydrophilicity of polymers. Therefore, when sulfated inorganic oxide nanoparticles are filled in polymer

membranes, there are MRLs inside channels and surface of membranes.

Based on the mentioned research and analysis, in order to investigate novel filler materials of composite membranes, TSANs can be fabricated through combining the advantages of SNT and sulfated TiO_2 solid superacid. TSANs have numerous hydroxyl active sites along the length direction of TSANs to be compatible with the polymers along the direction of PSF chains. Namely, O-H groups of TSANs interact with S=O double bond of PSF through S=O \cdots H-O hydrogen bond.²⁵ So when TSANs are doped into PSF to prepare TSANs/PSF composite membrane, some of the hydroxyl active sites existing on the surface and channels of the composite membrane can interact with water molecules through hydrogen bonds,²⁶ which can effectively inhibit organic pollutants (hydrocarbon and soluble oil etc.) and microbes from passing through composite membranes and enhance hydrophilic properties of membranes; alternatively, MRLs formed in channels and on the surface of polymer can decompose inorganic pollutants or restrain the formation of inorganic pollutants, which will further enhance the integrated properties of polymer membranes, such as hydrophilicity, anti-fouling and anti-compaction performance. Therefore, it can be concluded from above analysis that the acidity of TSANs is important to form MRLs in membranes. Moreover, the preparation conditions perform the important impact on the structure and properties of TSANs such as the acidity. Thereby, the effect of preparation conditions of TSANs on their acidity should be deeply investigated.

In this paper, the preparation conditions of TSANs such as the molar ratio of Ti/Si, the concentration of sulphuric acid aqueous solution, the dipping time in sulphuric acid aqueous solution and the calcination temperature etc are investigated and optimized in detail, the optimum preparation conditions are determined by Hammett acidity H_0 test method; TSANs and

TSANs/PSF composite membranes are studied by SEM, TEM, EDX, FT-IR, BET and contact angle of water etc. Meanwhile, the effect of doping TSANs on properties of polysulfone membrane is also evaluated and observed.

2. Experimental

2.1. Materials and reagents

Concentrated sulfuric acid (H_2SO_4 , AR grade, 98%) was purchased from Beijing Chemical Factory. Aqueous ammonia (NH_3 , AR grade, 25%) and dehydrated ethanol were obtained from Tianjin Guangfu Fine Chemicals Co., Ltd. Tetraethyl orthosilicate (TEOS, AR grade, the mass ratio of silica dioxide is 28%) and tartaric acid ($\text{C}_4\text{H}_4\text{O}_6$, AR grade, 99.5%) were offered by Tianjin Jiangtian chemical Co., Ltd and Tianjin NO.1 Chemical reagent Factory, respectively. Tetra-n-butyl Titanate (TBT, AR grade, 98.0%) was bought from Tianjin KemiO Chemical Reagent Co., Ltd. Polysulfone (PSF) was purchased from Dalian Polysulfone Co., Ltd, and its MW and polydispersity were 84,400Da and 1.37, respectively. N,N-dimethylacetamide (DMAC, AR grade, 94.6%) was bought from Tianjin KemiO Chemical Reagent Co., Ltd and Polyethylene glycol with average MW 400 Da (PEG400, AR grade, 95%) was supplied by Tianjin Bo di Chemical Co., Ltd.

2.2. Preparation of TSANs

TSANs with the length of 8 μm and the inner diameter of around 300 nm were prepared in our laboratory. The preparation approach is schematically shown in Fig. 1.

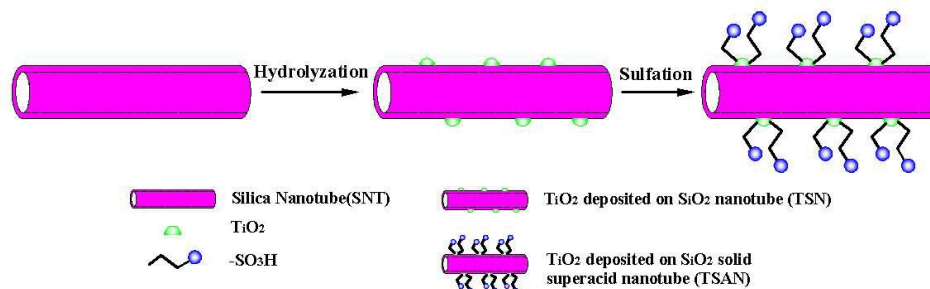


Fig. 1. Schematic diagram of preparation of TSANs

2.2.1. Preparation of SNTs.

SNTs were prepared by a template-guidance route, which is similar to the literature.²⁷ And the optimum preparation conditions of SNTs were determined as follows: the template is tartaric acid, the stirring rate is 300 rpm, the pre-reaction time is 15 min and the calcination temperature is 550°C. The detailed procedures are as follows: typically, TEOS was added to absolute ethanol containing tartaric acid and de-ionized water to prepare a mixed solution, and the mixture was allowed to stand for a while. Subsequently, 28% NH_4OH was added dropwise into the two reactors under stirring respectively, kept stirring for 10 min, and then the solution was left to stand for 2 h. The white precipitate was washed with a large amount of water to remove colloidal aggregates, centrifuged and dried at 60°C. At last the resulting particles were sintered at 550°C to obtain SNTs.

The whole SNTs samples applied in the below investigation were prepared under the above preparation conditions.

2.2.2. Preparation of TSNs.

SNTs were uniformly dispersed into anhydrous ethanol under stirring and intermittent ultrasound at 50°C. Then moderate TBT was added dropwise and slowly to above solution under

stirring to disperse uniformly. Subsequently, two drops of distilled water were added to the mixed solution and stirring was continued for 10 min. Then the reaction was completed after white precipitate was fully formed by standing the solution for 20 min. The white precipitate was repeatedly washed for three times with distilled water, followed by being centrifuged to get TSNs.

2.2.3. Sulfation of TSNs.

Finally, TSNs were immersed in appropriate concentration of sulphuric acid aqueous solution at appropriate time to be sulfated. And TSANs were obtained after calcined in a furnace for 4 h at a suitable calcination temperature.

2.3. Preparation of TSANs/PSF composite membranes

TSANs/PSF composite membranes were prepared by phase inversion methods.²⁸ Firstly, TSANs were added to DMAC in a 500ml flask under stirring at 60°. Then moderate PSF (the mass ratio of TSAN: PSF, 10: 100 (g: g)) was added and dissolved sufficiently under stirring and intermittent ultrasound. Two hours later, PEG 400 was added to the mixture as porogen to promote the yield of pores in the gelation process. Vigorous stirring was still needed to get a homogeneous solution. And then the solution was still kept for 24 h at 20 °C. The gel was cast on a horizontal glass plate to form composite membranes (thickness ca. 0.2mm) using a glass blade. After pre-evaporated 10 s in the air (25 °C and 60% relative humidity), composite membranes were immersed into a water bath at 50 °C. TSANs/PSF composite membranes were obtained after gel films fell off the glass plate. Finally, membranes were soaked in distilled water containing 1wt.% formaldehyde to avoid bacteria growth.

Pure PSF membranes, SiO₂/PSF and phosphorylated Zr-doped hybrid silica (SZP)/PSF composite membranes²⁸ were prepared by using the same procedures mentioned above, just

TSANs were replaced with nothing, SiO₂ (the mass ratio of SiO₂: PSF, 10: 100 (g: g)) and SZP (the mass ratio of SZP: PSF, 10: 100 (g: g)), respectively.

2.4. Characterization

The FT-IR spectra of SNTs, TSNs and TSANs samples were collected on an Avatar 370 spectrometer (Thermo Nicolet Corporation, USA), using the potassium bromide pellet technique. Its wavelength coverage was 4000-370 cm⁻¹ and distinguish ability was 0.1 cm⁻¹. TEM images of TSANs were recorded on a JEM-2100F II transmission electron microscope (JEOL Corporation, Japan) with the operating voltage of 100 KV. TEM samples were prepared by briefly ultrasonically dispersing powders in absolute ethanol, followed by placing a drop of suspension onto a carbon coated copper grid. The grids were desiccated before measurement. Cross-section samples were obtained by being freeze-fractured in liquid nitrogen to obtain a tidy cross-section and then sputtered with gold. The cross-section of SNTs and TSANs/PSF composite membrane were observed under a HITACHI S4800 scanning electron microscope using an accelerating voltage of 5 kV. The specific surface areas and pore size distributions of TSANs were determined by the BET method using a Micromeritics Instrument Corp. Tristar 3000 specific surface area analyzer.

2.5. Measurement of suspended solids decomposition rate

In order to prove TSANs/PSF composite membrane can decompose inorganic pollutants such as metal oxides, we investigated the decomposition rate of the composite membrane to suspended solids in oily sewage. Specific operation method and principle are as follows: a piece of microporous membrane was weighed accurately after vacuum drying to constant weight to record its weight, then it was put into a Buchner funnel. A certain volume of fluid solution at test was measured. A vacuum pump was kept open in the process of filtration, with plastic Turkey Baster

slowly dripping fluid solution at test into the microporous membrane. Finally, the microporous membrane used in the process of filtration was dried to constant weight to record its weight. The suspended solid of fluid solution at test was described as follows:

$$SS = \frac{A_2 - A_1}{V} \times 10^6 \quad (1)$$

where SS is the suspended solid of fluid solution at test (mg/L), A_1 the weight of fluid solution at test before filtration (g), A_2 the weight of fluid solution at test after filtration (g), V the volume of fluid solution at test (L). Therefore, the decomposition rate of suspended solids by composite membrane could be calculated by the following formula:

$$D_{ss} = \frac{(SS_0 - SS_2) - (SS_0 - SS_1)}{SS_0} \times 100\% \quad (2)$$

where D_{ss} is the decomposition rate of suspended solids in oily sewage (%), SS_0 is the initial suspended solids of oily sewage (mg/L), SS_1 is the remaining suspended solids of oily sewage (mg/L), which is adsorbed by PSF membrane, SS_2 is the remaining suspended solids of oily sewage (mg/L), which is adsorbed and decomposed by TSANs/PSF composite membrane.

2.6. Membrane separation performance studies

2.6.1. Preparation of wastewater containing oil

The model oily wastewater (oil-in-water emulsion) was created by machine oil and distilled water with vigorous stirring at 300 r/min speed over 1h until a homogeneous solution was obtained. The stability of the emulsion was observed visually over 24 h period and the mixture maintained cloudy and turbid, indicating that oil was in an emulsified and soluble condition. After treated by sand leach and fiber filtration, oil in the model sewage was incised and separated, which makes the model oily wastewater become the emulsions with different oil concentration. The oil concentration in the permeate was determined by a UV spectrophotometer (SP-752 UV-visible

spectrophotometer, Shanghai spectrum Corporation) at 225 nm. The absorbance of fluid under test could be converted to the value of oil concentration.

2.6.2. Ultrafiltration experiment

Ultrafiltration experiment of oily wastewater was carried out with PSF membranes, SiO₂/PSF composite membrane, SZP/PSF composite membrane and TSANs/PSF composite membrane, respectively. The membrane evaluation device was made in our laboratory. The operation condition of the separation experiments was an intermittent mode.

The oil retention of membranes was measured after the above experiment and the retention R is calculated by the following equation:

$$R = \frac{C_1 - C_2}{C_1} \times 100\% \quad (3)$$

where R is the retention (%), C₁ is the oil concentration in the feed solution (mg/L) and C₂ is the oil concentration in the permeation (mg/L).

3. Results and discussion

3.1. The optimum preparation conditions of TSANs

SNTs and silylation of SNTs during preparing TSANs had been studied in our previous investigation,²⁹ so in this paper the effect of preparation conditions of TSANs on the acidity of TSANs were researched, such as the molar ratio of Ti/Si, the different concentration of sulphuric acid aqueous solution, the dipping time in sulphuric acid aqueous solution and the calcination temperature etc. Based on the mentioned analysis, the reason is that the acidity of TSANs is of great significance to the formation of MRLs in membranes.

3.1.1. Effect of the molar ratio of Ti/Si on the acidity of TSANs.

In order to investigate the effect of the molar ratio of Ti/Si on the acidity of TSANs,

different molar ratios of Ti/Si (1:1, 1:2, 1:3, 1:4, 1:5 (mol: mol)) were studied and observed. As shown in Fig. 2, when the molar ratio of Ti/Si is 1:3, the acidity of TSANs reaches a maximum value (-7.584), which can promote the formation of MRLs in membranes. This is because the formation of MRLs is related to the acidity of TSANs.³⁰ Therefore, the optimum molar ratio of Ti/Si in the process of preparation of TSANs is 1:3.

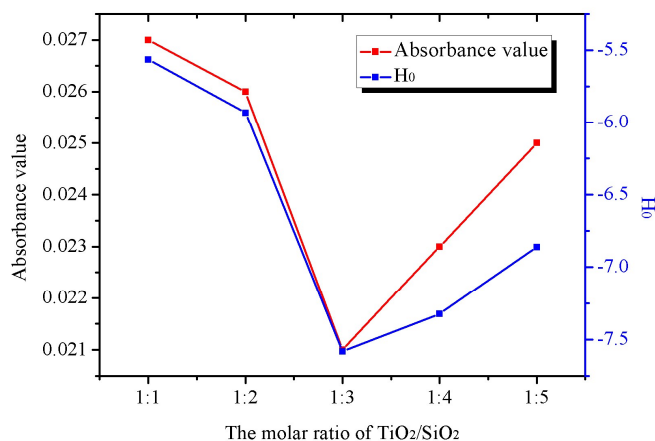


Fig. 2. The effect of the molar ratio of Ti/Si on the acidity of TSANs

3.1.2. Effect of concentration of H₂SO₄ aqueous solution on the acidity of TSANs.

In order to investigate the effect of concentration of H₂SO₄ aqueous solution on the acidity of TSANs, different concentration of H₂SO₄ aqueous solution (0.5 mol/L, 1.0 mol/L, 1.5 mol/L, 2.0 mol/L, 2.5 mol/L) were discussed when the molar ratio of Ti/Si was 1:3. As shown in Fig. 3, when the concentration of H₂SO₄ aqueous solution is 1.0 mol/L, the acidity of TSANs reaches a maximum value (-8.002). The reason is that when the concentration of H₂SO₄ aqueous solution is less than 1.0 mol/L, the acidity of TSANs indeed is smaller (-7.584) due to less SO₄²⁻ groups; alternatively, when the concentration of H₂SO₄ aqueous solution is more than 1.0 mol/L, the acidity of TSANs also becomes small, this is because a lot of SO₄²⁻ groups may clog the pores of the metal oxide and reduce the specific surface area, which reduces the acidity of TSANs.

Therefore, the optimum concentration of H_2SO_4 aqueous solution is 1.0 mol/L.

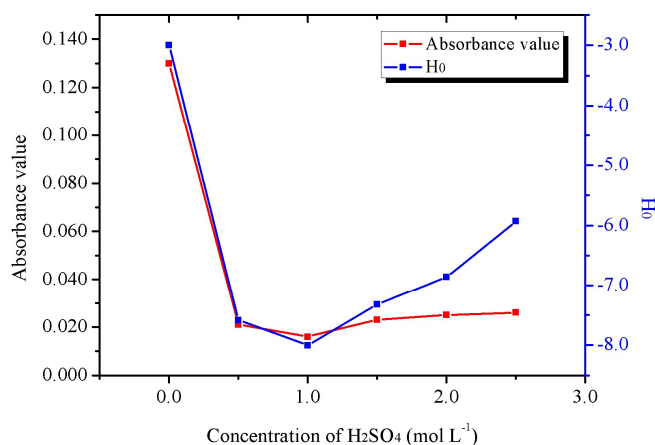


Fig. 3. The effect of concentration of H_2SO_4 aqueous solution on the acidity of TSANs

3.1.3. Effect of dipping time in H_2SO_4 aqueous solution on the acidity of TSANs.

The effect of dipping time in H_2SO_4 aqueous solution on the acidity of TSANs was studied by changing the dipping time of TSANs prepared based on the optimized preparation condition (the molar ratio of Ti/Si was 1:3 (mol: mol), the concentration of H_2SO_4 aqueous solution was 1.0 mol/L). As shown in Fig. 4, comparing the different dipping time in sulfating process, it can be observed that the acidity of TSANs increases gradually with the dipping time extends. However, when the dipping time exceeds 4 h, the acidity of TSANs reaches a steady state (-8.002). Therefore, the optimum dipping time of TSANs in H_2SO_4 aqueous solution is 4 h.

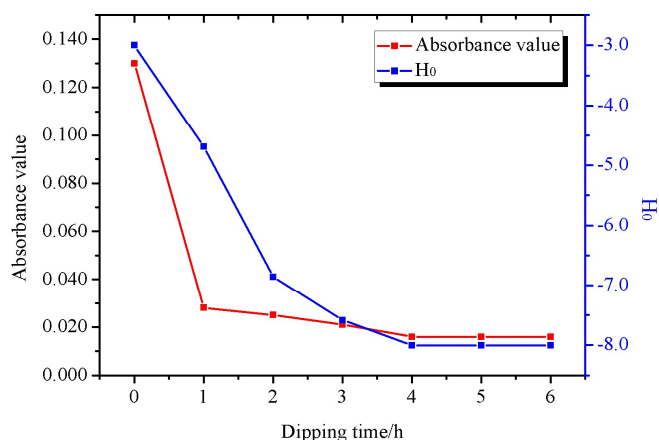


Fig. 4. The effect of dipping time in H_2SO_4 aqueous solution on the acidity of TSANs

3.1.4. Effect of calcination temperature on the acidity of TSANs.

The effect of calcination temperature after sulfation on the acidity of TSANs was studied by changing the calcination temperature of TSANs prepared based on the optimized preparation condition (the molar ratio of Ti/Si was 1:3 (mol: mol); the concentration of H_2SO_4 aqueous solution was 1.0 mol/L; the dipping time in sulphuric acid aqueous solution was 4 h). Fig. 5 represents the acidity of TSANs calcinated at different temperature for 4 h. As depicted in Fig. 5, when the calcination temperature is 600 °C, the acidity of TSANs reaches a maximum value (-7.687). The amorphous TiO_2 can be converted into tetragonal system (anatase type) with catalytic activities at 600 °C.³¹ Moreover, tetragonal system of TiO_2 can combine with SO_4^{2-} to form the solid superacid. So lower calcination temperature limits the formation of superacid center. In contrast, higher calcination temperature indeed causes the loss and decomposition of SO_4^{2-} ,³² which can not form the solid superacid. Therefore, the optimum calcination temperature of TSANs is 600°C.

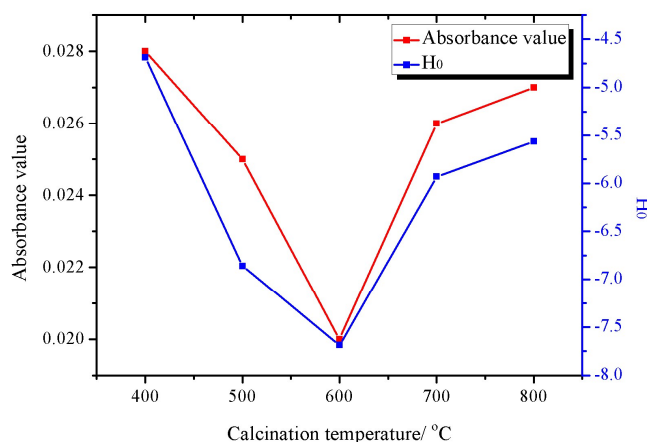


Fig. 5. The effect of calcination temperature on the acidity of TSANs

Based on the above discussion and analysis, the optimum preparation conditions of TSANs can be confirmed below: the molar ratio of Ti/Si is 1:3 (mol: mol), the concentration of H_2SO_4 aqueous solution is 1.0 mol/L, the dipping time in H_2SO_4 aqueous solution is 4h and the calcination temperature is 600 °C. TSANs prepared under optimum preparation conditions showed high acidity by Hammett acidity H_0 test, ensuring TSANs/PSF composite membranes formed by doping TSANs had MRLs inside channels and on the surface of membranes. The formation of MRLs further enhanced the integrated properties of PSF membranes such as hydrophilicity, anti-fouling and anti-compaction performance.

3.2. The SEM analysis of SNTs

Fig. 6 shows SEM images of the cross-section of SNTs synthesized under the above optimum preparation conditions. It can be seen from Fig. 6 that SNTs have tubular structure and their wall is extremely smooth and the nanotubes are translucent. Alternatively, the physical properties of SNTs are as follows: the inner diameter of SNTs is about 300~400 nm, the thickness of the tube wall is about 50 nm.

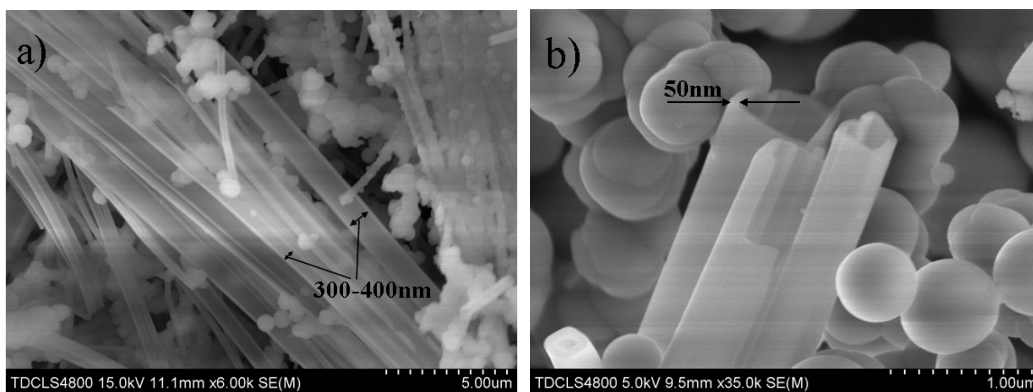


Fig. 6. SEM images of SNTs [magnification: a) $\times 6000$; b) $\times 35000$]

3.3. The TEM analysis of TSANs

Fig. 7 displays TEM images of TSANs synthesized under the optimum preparation conditions. As can be seen from Fig. 7, TSANs have tubal structure characteristic, the length of TSANs is approximately 8 μm , the inner diameter of TSANs is 350 nm, the thickness of the tube wall is 50 nm and the ratio of length to diameter of TSANs is approximately 23. Moreover, it can be also observed from Fig. 7 that the tube wall of TSANs is not so smooth as SNTs. The reason is that TiO_2 nanoparticles have been deposited on SiO_2 nanotubes.

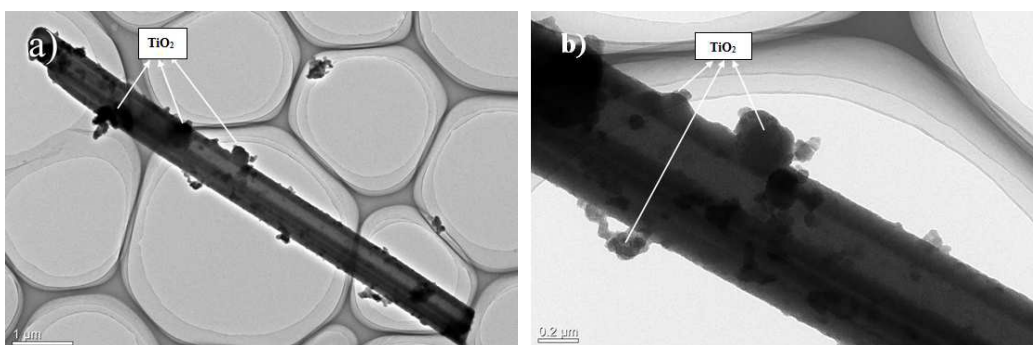


Fig. 7. TEM images of TSANs [magnification: a) $\times 1500$; b) $\times 5000$]

3.4. The EDX analysis of TSANs

Fig. 8 is the EDX spectrum of TSANs prepared under the optimum preparation conditions. It can be seen from the EDX spectrum of TSANs that the existence of Si, Ti, O and S elements can be found obviously. And the presence of C and Cu elements can be found. That is because TSAN

samples were prepared by briefly ultrasonically dispersing powders in absolute ethanol, followed by placing a drop of suspension onto a carbon coated copper grid. The relative content of elements in TSANs is shown in Table 1. It can be obtained from Table 1 that the molar ratio of Ti/Si is about 1:3 (mol: mol), which conforms to the optimum preparation conditions.

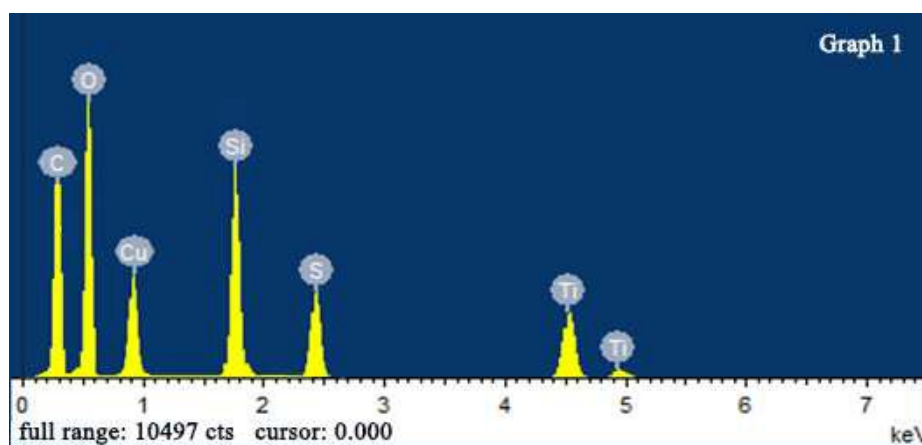


Fig. 8. The EDX spectrum of TSANs

Table 1

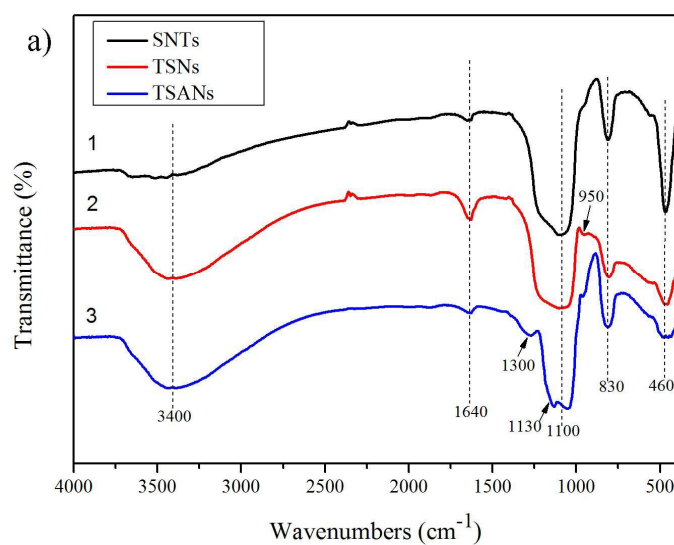
The relative content of elements in TSANs

Elements	Weight percent (%)	Atomic percent (%)
O K	36.17	44.25
Si K	20.25	14.16
C K	18.99	30.97
Ti K	10.85	4.42
Cu K	7.23	2.21
S K	6.51	3.99
Total	100.00	100

3.5. The FT-IR analysis of TSANs

The infrared spectra of SNTs, TSNs and TSANs are shown in Fig. 9. It can be observed from the infrared spectra of three kinds of particles that absorption peaks which appear at 1100 cm^{-1} ,

830 cm^{-1} and 460 cm^{-1} are the asymmetric stretching vibration peak, symmetric stretching vibration peak and bending vibration peak of Si-O-Si, respectively.³³⁻³⁵ They indicate that the main structures of these materials are silica. Both of the peaks at 3400 cm^{-1} and 1640 cm^{-1} (stretching vibration peak and bending vibration peak of O-H) on the second and third spectrum are obviously larger than the first one.^{25, 36} This indicates that there are abundant hydroxide radicals on the surfaces of TSNs and TSANs, which means that the hydrophilicity of SNTs has increased after the deposition of sulfated TiO_2 . In the infrared spectra of TSNs, the stretching vibration peak of Si-O-Ti appears at 950 cm^{-1} ,³⁷ which manifests that TiO_2 has been deposited on SNTs successfully. As can be seen from Fig. 9 b), the absorption peak appearing at 1300 cm^{-1} on the third spectrum is the stretching vibration of S=O bond and the absorption peak near 1130 cm^{-1} is the characteristic vibration of the Ti-O-S bond, indicating that a chemical bond (Ti-O-S bond) between SO_4^{2-} and TiO_2 is formed.³⁸⁻³⁹ Therefore, the FT-IR results clearly indicate that sulphate has been grafted to TiO_2 successfully and TSANs have been formed.



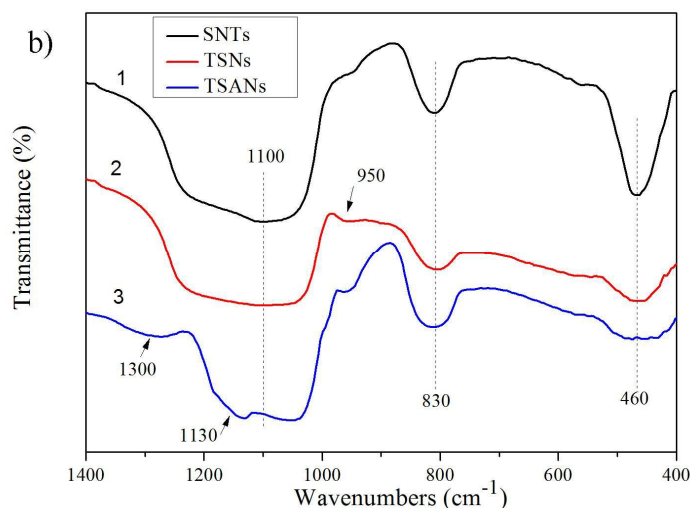


Fig. 9. The FT-IR spectrum of SNTs, TSNs and TSANs [a) Wavenumbers: 400-4000 cm^{-1} ; b) Wavenumbers: 400-1400 cm^{-1}]

3.6. The BET analysis of TSANs

Specific surface area and pore size distribution of TSANs synthesized under the above optimum preparation conditions are examined by Brunauer-Emmett-Teller (BET) and Barrett-Joyner-Halenda (BJH) methods, respectively. The specific surface area of TSANs is $480.2\text{m}^2/\text{g}$. Fig. 10 shows the nitrogen adsorption-desorption isotherm and pore size distribution of TSANs. It can be observed from Fig. 10 that TSANs show type IV adsorption characteristics and a hysteresis loop of type H1 appears owing to nitrogen adsorption of tubular pores of TSANs. As can be seen from Fig. 10, the nitrogen adsorption isotherm has two peaks, which indicates that TSANs have two sorts of pore sizes. Fig. 10 indicates that the pore size of TSANs presents double distribution; the pores whose average pore size is 7.4 nm attribute mesopores of the tube wall of TSANs while the pores whose average pore size is 350 nm attribute the tubular inner pores of TSANs.

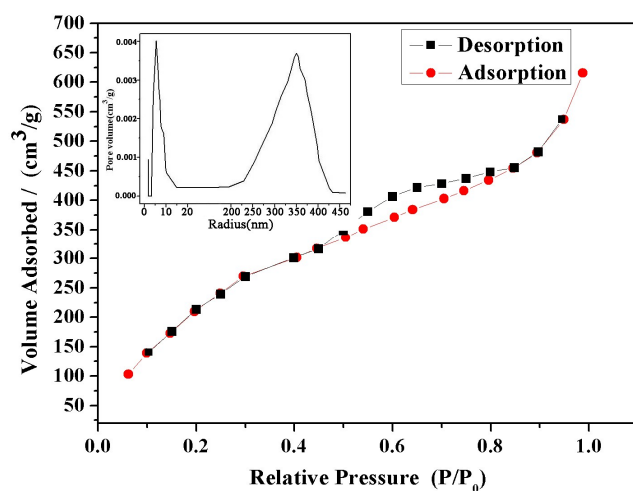


Fig. 10. Nitrogen adsorption - desorption isotherm and BJH pore size distribution of TSANs

3.7. SEM studies of composite membrane

Fig. 11 shows SEM images of the cross-section of TSANs/PSF composite membranes prepared by doping TSANs to PSF membrane. In Fig. 11a), TSANs/PSF composite membranes have the asymmetric structure with compact skin layer and porous support substrate. The skin layer can hold back macromolecular substance for its compact property and let rinsing get through, while the substrate with numerous finger-like cavities along the entire membrane thickness functions as anti-compaction supporting layer. It can be observed from Fig. 11b) that TSANs are dispersed inside PSF membranes uniformly, which can form MRLs inside channels and surface of membranes. Alternatively, it can also be seen that TSANs and PSF polymer chains combine well, which increases the anti-compaction ability and hydrophilicity of PSF polymer membranes, enhancing the integrative properties of TSANs/PSF membranes.

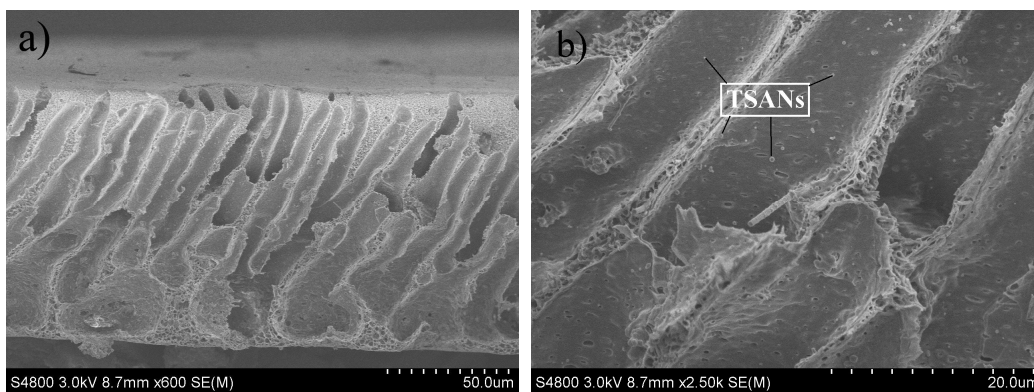


Fig. 11. SEM images of the cross-section of TSANs/PSF composite membranes

[magnification: a) $\times 600$; b) $\times 2500$;

3.8. The hydrophilic property analysis of TSANs/PSF composite membrane

The relative hydrophilicity of membrane surface can be easily obtained by water contact angle measurement,⁴⁰ namely a membrane with a lower water contact angle exhibits a better hydrophilic property. The contact angles between water droplet and PSF composite membranes doping different inorganic particles were tested. It can be observed from Fig. 12 and Fig. 13 that the contact angle of TSANs/PSF composite membranes is the smallest of 36.5° , which indicates that the hydrophilicity of TSANs/PSF composite membranes is better than the other three composite membranes. This is because sulfated TiO_2 solid superacid with strong acidity can form hydrophilic surroundings on the surface of PSF membranes; alternatively, in the length direction of TSANs, more hydroxide radicals are supplied by S-OH, Ti-OH and a lot of Lewis acid sites, ensuring the formation of many hydrogen bonds between aqueous solution and TSANs. Therefore, TSANs/PSF composite membranes show stronger hydrophilic property.

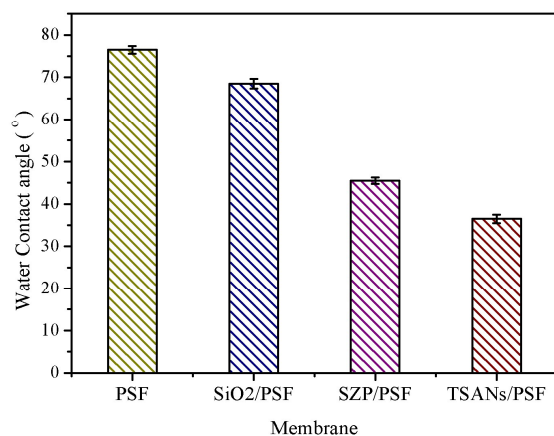


Fig. 12. The effect of different particles on membrane hydrophilicity

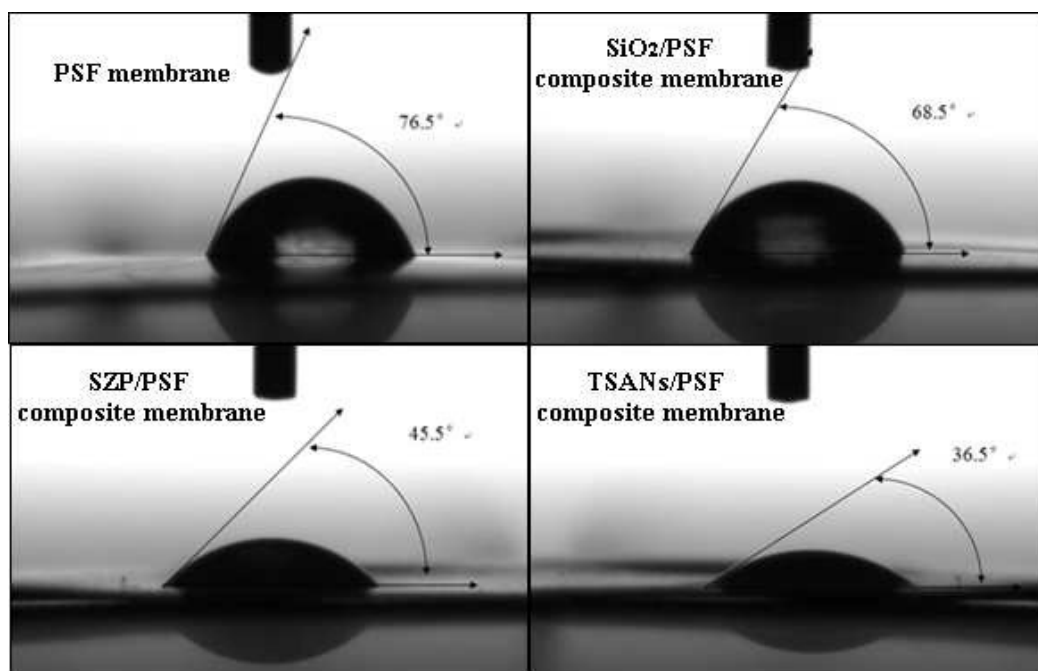


Fig. 13. Contact angles of different membranes

3.9 Anti-compaction performance studies

Section S3 in supplementary information shows the measurement method of membrane anti-compaction performance. Fig. 14 shows the effect of different doping materials on the membrane ultrafiltration water permeation flux of membranes (under pressure of 0.10 MPa, temperature of 25°C). In Fig. 14, it is observed that the membrane ultrafiltration water permeation

flux of TSANs/PSF composite membrane is bigger than that of PSF membrane, SiO₂/PSF composite membrane and SZP/PSF composite membrane. Meanwhile, the incrementation between membrane ultrafiltration water stable fluxes of TSANs/PSF composite membranes reaches a maximum of 425.35 % as the data indicated in Table 2, which indicates that membrane ultrafiltration water stable flux of TSANs/PSF composite membranes is more than four times of that of PSF membranes. These can be ascribed to the interaction between TSANs and PSF chains. On the one hand, SNTs with tubular structure, high specific surface areas and high ratio of length to diameter could be compatible well with polymers and the unique circular wall with nanometer thickness of TSANs can function as a new energy dissipation approach to resist the outer force effects. On the other hand, abundant of hydroxide radicals on the surface of TSANs can interact with PSF chains by hydrogen bonds. Thus, the anti-compaction property of PSF membranes is improved obviously by doping TSANs.

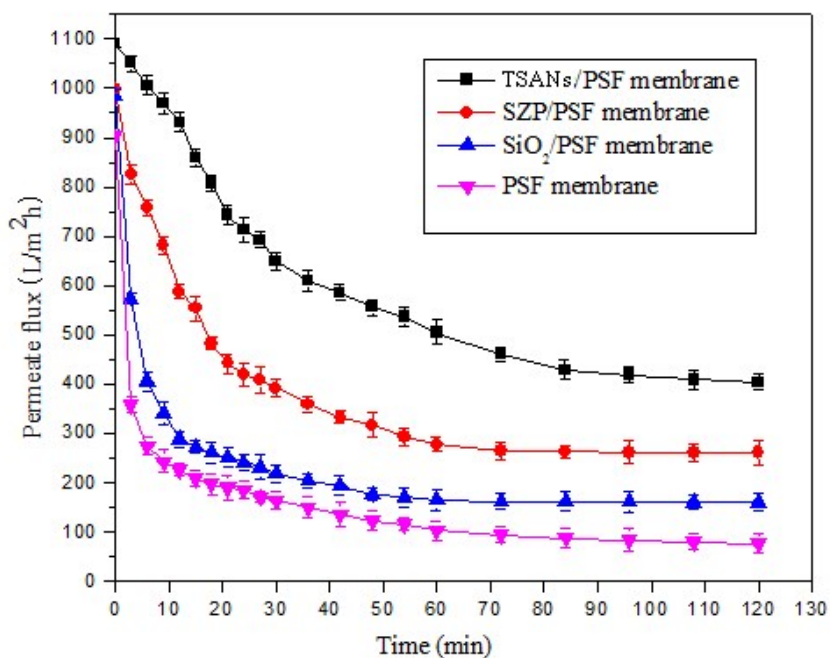


Fig. 14. The effect of different doping materials on the pure water permeation flux of membranes

Table 2

The incrementation between pure water stable fluxes of membranes

Membrane	Pure water stable fluxes (L/ m ² h)	Incrementation between pure water stable fluxes (%)
PSF membrane	77	0
SiO ₂ /PSF composite membrane	161	109.09
SZP/PSF composite membrane	261	238.96
TSANs/PSF composite membrane	404	424.67

3.10. Effect of different doped materials on separation properties of membranes

In order to investigate the effect of different doped materials on separation performance of membranes, ultrafiltration experiments of wastewater containing oil (oil concentration 71.46 mg/L, operating temperature 25°C, operating pressure 0.1 MPa) were carried out with PSF membranes, SiO₂/PSF composite membranes, SZP/PSF composite membranes and TSANs/PSF composite membranes, respectively. Fig. 15 shows the effect of different doped materials on permeation flux of membranes when treated wastewater containing oil. It can be observed from Fig. 15 that TSANs/PSF composite membranes show a higher stable flux of 113 L/m²h than other three membranes. Table 3 shows the oil retention rate of these four membranes. Among all the membranes, TSANs/PSF composite membranes show the attractive oil retention property and its oil retention rate reaches 94.2 %. The above results indicate that TSANs/PSF composite membrane has better separation performance. It is because the stronger hydrophilic surroundings inside channels and surface of membranes lead to form a water layer on the membrane surface⁴¹ and more hydroxide radicals can interact with water molecule by hydrogen bonds, which makes water molecule pass through pore channel smoothly while most of oil droplets and suspend solids

are intercepted by the membranes. Alternatively, MRLs formed in channels and on the surface of TSANs/PSF composite membrane can decompose inorganic pollutants or restrain the formation of inorganic pollutants. Meanwhile, there are many accessible active sites to be compatible with PSF membrane along the direction of polymer chains; in the diameter direction of TSANs, there is a unique circular wall with nanometer thickness, which can function as a new energy dissipation approach to resist the outer impact forces. Thereby, TSANs /PSF composite membranes show better compatibility, tensile strength and anti-compaction performance. From above research and analysis it can be known that TSANs with super strong acid, tubular structure and high ratio of length to diameter are firstly prepared, and then dope them to PSF to prepare TSANs/PSF composite membranes, making TSANs/PSF composite membranes have higher flux and attractive integrative properties and are suitable in application for treating wastewater.

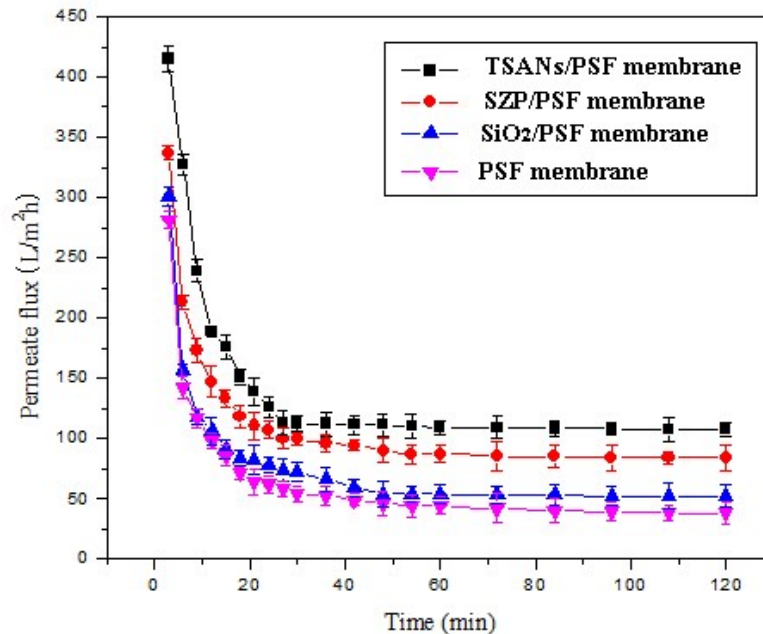


Fig. 15. The effect of doping different particles on membrane permeate flux

Table 3

The effect of different particles on membrane oil retention

Membrane	Oil concentration in permeation (mg/L)	Oil retention rate(%)
PSF membrane	5.47	92.3
SiO ₂ /PSF composite membrane	5.06	92.9
SZP/PSF composite membrane	4.61	93.5
TSANs/PSF composite membrane	4.15	94.2

3.11 Decomposition of TSANs/PSF composite membrane for inorganic pollutants

In order to prove TSANs/PSF composite membrane can decompose inorganic pollutants such as metal oxides, we investigated the decomposition rate of the composite membrane to suspended solids in oily sewage. The decomposition rate of TSANs/PSF composite membranes for suspended solids in oily sewage was calculated by the Eq. (2) and shown in Fig. 16. As indicated in Fig. 16, the decomposition rate of TSANs/PSF composite membranes for inorganic pollutants reaches 15.53% when the decomposition experiment of inorganic pollutants has been carried out for 120 min. The reason is that TSANs/PSF composite membranes have a lot of MRLs inside their channels and surfaces, a strong acid center of solid superacid is formed on the surface of TSANs, causing low pH and hydrophilic surroundings on the surface of PSF membranes. It makes inorganic pollutants hard to adhere on the surface of membranes. Although some inorganic pollutants can be absorbed on the surface or channels of membranes, these pollutants would be decomposed by strong acid center of TSANs. Therefore, in the process of TSANs/PSF composite membranes treating oily sewage, inorganic pollutants can be partially decomposed, achieving the aim of improving anti-fouling property of PSF membranes.

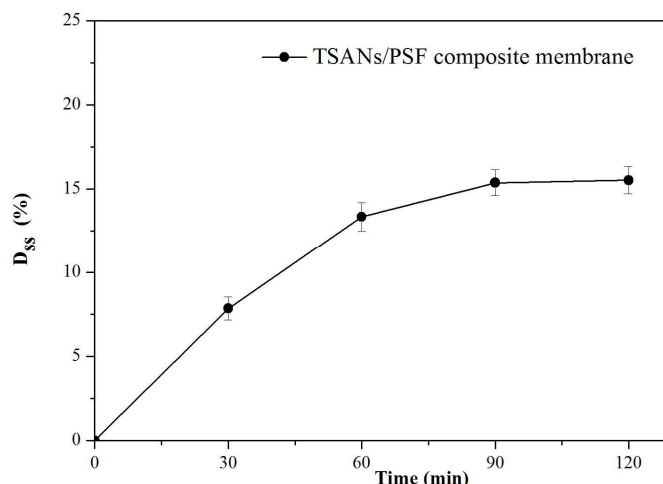


Fig. 16. Decomposition rate of inorganic pollutants by TSANs/PSF composite membrane

3.12. Analysis of the formation mechanism of MRLs inside channels and surface of TSANs/PSF composite membranes

3.12.1 The mechanism of interaction between TSANs and PSF chains

Fig. 17 presents a mechanism scheme of the interaction between TSANs and PSF chains. As indicated in Fig 17, TSANs have numerous hydroxyl active sites along the length direction of TSANs to be compatible with the polymers along the direction of PSF chains. These hydroxyl groups can interact with PSF chains by hydrogen bonds. Namely, O-H groups of TSANs interact with S=O double bond of PSF through S=O \cdots H-O hydrogen bond. Alternatively, in the diameter direction of TSANs, there is a unique circular wall with nanometer thickness, which can function as a new energy dissipation approach to resist the outer impact forces. It ensures that TSANs/PSF composite membranes have good anti-compaction property.

3.12.2 The formation scheme of MRLs inside channels and surface of TSANs/PSF composite membranes

Fig. 18 presents the formation scheme of MRLs. The process of inorganic pollutants degraded by TSANs/PSF composite membrane is shown in this figure. A strong acid center of

solid superacid was formed on the surface of TSANs, causing low pH and hydrophilic surroundings on the surface of PSF membranes. It makes inorganic pollutants hard to adhere on the surface of membranes. Although some inorganic pollutants can be absorbed on the surface or channels of membranes, these pollutants would be degraded by strong acid center of TSANs or without forming these pollutants around strong acid center of TSANs. These results make TSANs/PSF composite membranes have good anti-inorganic fouling properties. Moreover, some of the hydroxyl active sites existing on the surface and channels of the composite membrane can interact with water molecules through hydrogen bonds, which can effectively inhibit organic pollutants (hydrocarbon and soluble oil etc.) and microbes from passing through composite membranes and enhance hydrophilic properties of membranes.

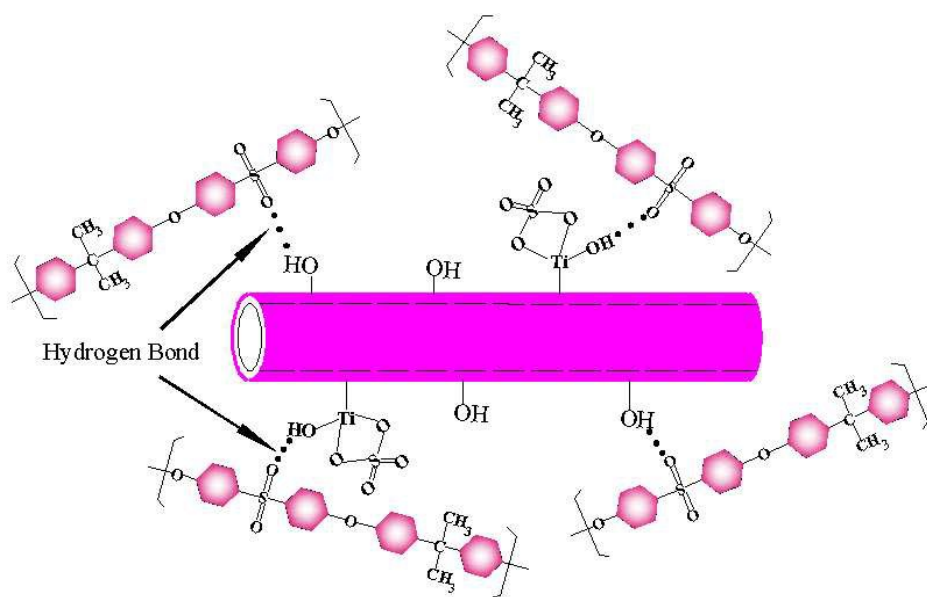


Fig. 17. The mechanism of interaction between TSANs and PSF chains

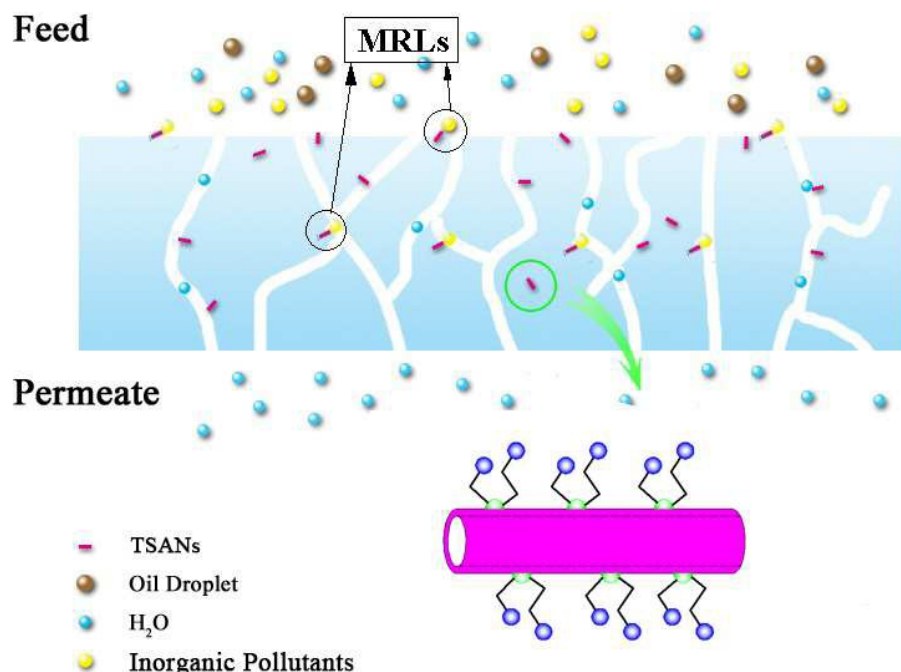


Fig. 18. The formation scheme of MRLs inside channels and surface of TSANs/PSF composite membranes

4. Conclusions

In this paper, the optimum preparation conditions of TSANs were investigated and determined, and then doped TSANs into PSF to prepare a TSANs/PSF composite membrane. The optimum preparation conditions of TSANs are: the molar ratio of Ti/Si is 1:3 (mol: mol), the concentration of H₂SO₄ aqueous solution is 1.0 mol/L, the dipping time in H₂SO₄ aqueous solution is 4 h and the calcination temperature is 600 °C. The results of SEM, TEM, EDX, FT-IR, BET and contact angle of water indicate that TSANs with high acidity are successfully prepared, and TSANs can be dispersed well in PSF membrane, making TSANs/PSF composite membranes not only have better compatibility but also have a lot of MRLs inside channels and surface of membranes. The formation of MRLs can further enhance the integrated properties of PSF

membranes, such as hydrophilicity, anti-fouling and anti-compaction performance. Therefore, TSANs are desirable as novel filler materials of polysulfone membrane.

Abbreviations

TSANs TiO_2 deposited on SiO_2 solid superacid nanotubes

MRLs micro reaction locations

PSF polysulfone

CNTs carbon nanotubes

SNTs silica nanotubes

TSNs TiO_2 deposited on SiO_2 nanotubes

SZP phosphorylated Zr-doped hybrid silica

Notation

H_0 Hammett acidity

SS suspended solid of fluid solution at test (mg/L)

A_1 weight of fluid solution at test before filtration (g)

A_2 weight of fluid solution at test after filtration (g)

V volume of fluid solution at test (L)

D_{SS} decomposition rate of suspended solids in oily sewage (%)

SS_0 initial suspended solids of oily sewage (mg/L)

SS_1 remaining suspended solids of oily sewage (mg/L)

R retention (%)

C_1 oil concentration in the feed solution (mg/L)

C_2 oil concentration in the permeation (mg/L)

Acknowledgments

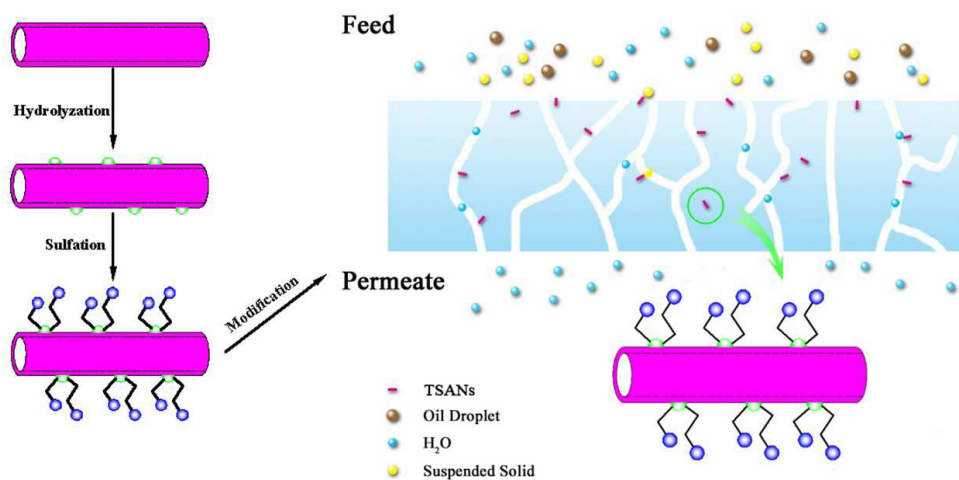
This project is supported by National Natural Science Foundation of China (No. 21076143), by the key technologies R & D program of Tianjin (15ZCZDSF00160), by the Basic Research of Tianjin Municipal Science and Technology Commission (13JCYBJC20100), by Tianjin Municipal Science and Technology Xinghai Program (No.KJXH2014-05), by State Key Laboratory of Chemical Engineering (No. SKL-ChE- 15B03).

References

- 1 H.J. Song and C.K. Kim, *J. Membr. Sci.*, 2013, **444**, 318-326.
- 2 V.R. Pereira, A.M. Isloor, U.K. Bhat, A.F. Ismail, A. Obaid and H.-K. Fun, *RSC Adv.*, 2015, **5**, 53874-53885.
- 3 E. Eren, A. Sarihan, B. Eren, H. Gumus and F.O. Kocak, *J. Membr. Sci.*, 2015, **475**, 1-8.
- 4 H.-B. Dong, Y.-Y. Xu, Z. Yi and J.-L. Shi, *Appl. Surf. Sci.*, 2009, **255**, 8860-8866.
- 5 S.B. Teli, S. Molina, A. Sotto, E.G. Calvo and J.d. Abajob, *Ind. Eng. Chem. Res.*, 2013, **52**, 9470-9479.
- 6 G. Zhang, S. Lu, L. Zhang, Q. Meng, C. Shen and J. Zhang, *J. Membr. Sci.*, 2013, **436**, 163-173.
- 7 Y. Yang, H. Zhang, P. Wang, Q. Zheng and J. Li, *J. Membr. Sci.*, 2007, **288**, 231-238.
- 8 A. Ahmad, M. Majid and B. Ooi, *Desalination*, 2011, **268**, 266-269.
- 9 Y.M. Mojtahedi, M.R. Mehmnia and M. Homayoonfal, *Desalin. Water Treat.*, 2013, **51**, 6736-6742.
- 10 S. Iijima, *Nature*, 1991, **354**, 56-58.
- 11 Ihsanullah, A.M. Al Amer, T. Laoui, A. Abbas, N. Al-Aqeeli, F. Patel, M. Khraisheh, M.A. Atieh and N. Hilal, *Mater. Des.*, 2016, **89**, 549-558.

- 12 C.-M. Chang, H.-Y. Li, J.-Y. Lai and Y.-L. Liu, *RSC Adv.*, 2013, **3**, 12895-12904.
- 13 S.A.R. Hashmi, H.C. Prasad, R. Abishera, H.N. Bhargaw and A. Naik, *Mater. Des.*, 2015, **67**, 492-500.
- 14 H.J. Fan, U. G02sele and M. Zacharias, *Small*, 2007, **3**, 1660-1671.
- 15 K.-S. Kim and S.-J. Park, *Electrochim. Acta*, 2012, **78**, 147-153.
- 16 C. Gao, Z. Lu and Y. Yin, *Langmuir*, 2011, **27**, 12201-12208.
- 17 N. Esman, A. Peled, R. Ben-Ishay, Y. Kapp-Barnea, I. Grigoriants and J.-P. Lellouche, *J. Mater. Chem.*, 2012, **22**, 2208-2214.
- 18 A. Nan, X. Bai, S.J. Son, S.B. Lee and H. Ghandehari, *Nano Lett.*, 2008, **8**, 2150-2154.
- 19 W. Gao, H. Liang, J. Ma, M. Han, Z.-l. Chen, Z.-s. Han and G.-b. Li, *Desalination*, 2011, **272**, 1-8.
- 20 W. Zhang, W. Liang, G. Huang, J. Wei, L. Ding and M.Y. Jaffrin, *RSC Adv.*, 2015, **5**, 48484-48491.
- 21 C.-H. Yu, L.-C. Fang, S.K. Lateef, C.-H. Wu and C.-F. Lin, *J. Hazard. Mater.*, 2010, **177**, 1153-1158.
- 22 A. Sayari, S. Hamoudi and Y. Yang, *Chem. Mater.*, 2005, **17**, 212-216.
- 23 T. Jiang, Q. Zhao, M. Li and H. Yin, *J. Hazard. Mater.*, 2008, **159**, 204-209.
- 24 Z. Li, R. Wnetrzak, W. Kwapinski and J.J. Leahy, *ACS Appl. Mater. Interfaces*, 2012, **4**, 4499-4505.
- 25 O. Lukin, A. Shivanyuk, V.V. Pirozhenko, I.F. Tsymbal and V.I. Kalchenko, *J. Org. Chem.*, 1998, **63**, 9510-9516.
- 26 L. Scatena, M. Brown and G. Richmond, *Science*, 2001, **292**, 908-912.

- 27 F. Miyaji, S.A. Davis, J.P.H. Charmant and S. Mann, *Chem. Mater.*, 1999, **11**, 3021-3024.
- 28 Y. Zhang, Z. Jin, Y. Wang and P. Cui, *J. Membr. Sci.*, 2010, **361**, 113-119.
- 29 Y. Zhang, Y. Xu, Y. Lu, L. Zhao and L. Song, *Nanotechnology*, 2013, **24**, 315701.
- 30 Y. Zhang and P. Liu, *Chem. Eng. Sci.*, 2015, **135**, 67-75.
- 31 H. Yang, R. Lu and L. Wang, *Mater. Lett.*, 2003, **57**, 1190-1196.
- 32 F. Zane, S. Melada, M. Signoretto and F Pinna, *Appl. Catal., A*, 2006, **299**, 137-144.
- 33 V.A. Zeitler and C.A. Brown, *J. Phys. Chem.*, 1957, **61**, 1174-1177.
- 34 K.Y. Jung and S.B. Park, *Appl. Catal. B: Environ.*, 2000, **25**, 249-256.
- 35 H. Xiong, S. Tang, H. Tang and P. Zou, *Carbohydr. Polym.*, 2008, **71**, 263-268.
- 36 L. Fang, X. Zu, Z. Li, S. Zhu, C. Liu, W. Zhou and L. Wang, *J. Alloys Compd.*, 2008, **454**, 261-267.
- 37 Y. Song, Y. Hasegawa, S. Yang and M. Sato, *J. Mater. Sci.*, 1988, **23**, 1911-1920.
- 38 L. Yan, W. Li, Z. Qi and S. Liu, *J. Polym. Res.*, 2006, **13**, 375-378.
- 39 D. S. Guo, Z.F. Ma, Q. Z. Jiang, H. H. Xu, Z. F. Ma and W. D. Ye, *Catal. Lett.*, 2006, **107**, 155-159.
- 40 F. Liu, B.-K. Zhu and Y.-Y. Xu, *Appl. Surf. Sci.*, 2006, **253**, 2096-2101.
- 41 B. Chakrabarty, A. Ghoshal and M. Purkait, *Chem. Eng. J.*, 2010, **165**, 447-456.



TSANs were employed as novel filler materials to prepare TSANs/PSF composite membranes with MRLs, improving the integrated properties of membrane.